EUROPHYSICS LETTERS 1 June 2003

Europhys. Lett., **62** (5), pp. 732–738 (2003)

Presence of a paramagnetic phase well below the ferromagnetic onset in $La_{0.67-x}Bi_xCa_{0.33}MnO_3$

J. R. Sun[1], B. G. Shen[1], J. Gao[2], Y. Fei[3] and Y. P. Nie[4]

[1] *State Key Laboratory for Magnetism, Institute of Physics and Center for Condensed Matter Physics, Chinese Academy of Sciences - Beijing 10080, PRC*

[2] *Department of Physics, the Hong Kong University - Pokfulam Road, Hong Kong, PRC*

[3] *Australian Nuclear Science and Technology Organization, Lucas Heights, Laboratories Menai 2234, Australia*

[4] *Department of Physics, Sichuan University - Chengdu 19904, PRC*

(received 21 January 2003; accepted in final form 4 April 2003)

PACS. 75.50.Dd – Nonmetallic ferromagnetic materials.
PACS. 76.30.-v – Electron paramagnetic resonance and relaxation.
PACS. 75.30.Vn – Colossal magnetoresistance.

Abstract. – Partial replacement of La by Bi in $La_{0.67}Ca_{0.33}MnO_3$ depresses the ferromagnetic order of the compound and leads to a stepwise magnetic behavior characterized by two subsequent transitions at $\sim 120\,K$ and $\sim 225\,K$. Based on a combined study of the electron spin resonance spectra and the thermal and isothermal magnetization, a complete scenario for the phase separation that causes the complex behavior has been given. It is found that the paramagnetic phase exists in a wide temperature region even below the ferromagnetic onset at $\sim 225\,K$. It coexists with the ferromagnetic phase below $\sim 240\,K$ and with both the ferromagnetic and antiferromagnetic phases below $\sim 190\,K$ with a reduced but significant fraction. The magnetization jump at $\sim 120\,K$ is possibly a conversion of the remaining paramagnetic phase into the ferromagnetic phase.

Partially replacing La in $La_{0.67}Ca_{0.33}MnO_3$ with Bi, Nd or Pr can result in dramatic magnetic and transport behaviors [1–6]. Instead of the simple paramagnetic (PM) to ferromagnetic (FM) transition, the compound will exhibit two magnetic transitions, respectively, at $T_c(H) \approx 220\,K$ and $T_c(L) \approx 110\,K$, which yields a novel stepwise increase of magnetization. As proved by a large body of evidence, this is a consequence of the coexistence and competition of charge-ordered (CO) antiferromagnetic (AFM) phase and FM phase. The magnetic onset at $T_c(H)$ is a conventional PM to FM transition followed by an AFM transition at a little lower temperature [6]. Therefore, it is generally believed that the FM and AFM phases coexist between $T_c(H)$ and $T_c(L)$. In contrast, the low-temperature transition is unordinary. A widely accepted opinion is that the AFM phase becomes unstable at low temperature and part of it is converted into the FM phase at $T_c(L)$ [3–6]. However, a recent study indicated that the volume fraction of the CO phase did not show any visible changes passing through $T_c(L)$ [7, 8]. This yields a question about the origin and the nature of the low-temperature transition. A natural assumption is that the magnetic jump at $T_c(L)$ is also a PM-FM, instead

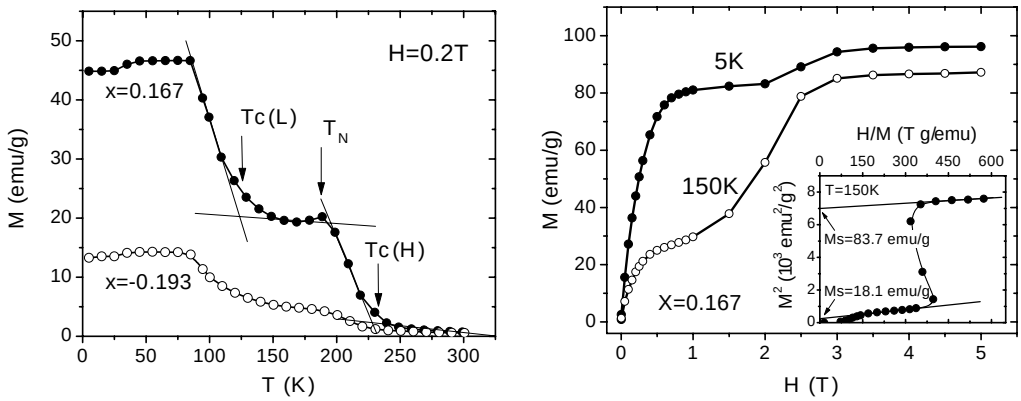

Fig. 1 – Temperature-dependent magnetization (left panel) and isothermal magnetization (right panel) of $La_{0.67-x}Bi_xCa_{0.33}MnO_3$. The bottom inset shows the Arrott plot of LBCM8. The definitions of T_c(H) and T_c(L) are also given in the figure. T_N denotes the temperature for the antiferromagnetic transition. The solid lines are guides for the eye.

of an AFM-FM, transition. This, in fact, postulates the presence of PM phase in the temperature region ~ 100 K below T_c(H) and the two-step manner of the PM-FM transition. Though PM phase has been reported to exist below the Curie temperature in $La_{0.67}Ca_{0.33}MnO_3$, its proportion decreases rapidly with cooling and completely vanishes ~ 20 K below T_c [9]. Therefore, whether the PM phase can subsist well below T_c(H) in the manganites showing stepwise magnetization is still an open question. In this letter, by a careful study of the electron spin resonance (ESR) spectra, combined with neutron diffraction and other conventional magnetic measurement techniques, we tried to give a direct evidence for the presence of the PM phase in $La_{0.67-x}Bi_xCa_{0.33}MnO_3$ ($x = 0.167$) between T_c(H) and T_c(L).

Two polycrystalline samples of $La_{0.67-x}Bi_xCa_{0.33}MnO_3$ with $x = 0.167$ (LBCM8) and 0.193 (LBCM9) were prepared by the conventional solid-state reaction method following the procedure described elsewhere [1]. Phase purity and crystal structure of the samples were examined by X-ray diffraction using a Rigaku X-ray diffractometer with a rotating anode and Cu K_α radiation. ESR spectra were measured using a Bruker ER-200D spectrometer operated at a frequency of 9.5 GHz. Neutron diffraction was conducted on a Medium Resolution Powder Diffractometer at the Australian Nuclear Science and Technology Organization for selected temperatures between 5 K and 300 K. A quantum design magnetometer (SQUID) was used for the magnetic measurement. All the data were collected in the warming process.

Based on the Rietveld analysis of the X-ray diffraction data, the samples are single phase of orthorhombic structure with the *Pbnm* symmetry. The lattice parameters are $a = 5.4549$, $b = 5.4493$ and $c = 7.6981$ Å for LBCM8 and $a = 5.4525$, $b = 5.4511$, and $c = 7.6903$ Å for LBCM9. The incorporation of Bi yields a slight shrinkage of the unit cell compared to $La_{0.67}Ca_{0.33}MnO_3$ ($a = 5.4717$, $b = 5.4569$, and $c = 7.7112$ Å [10]). Figure 1 shows the temperature-dependent magnetization measured under a field of 0.2 T (left panel). It confirms the occurrence of a stepwise magnetic behavior. The system first undergoes a PM to FM transition at T_c(H) ≈ 225 K, which leads it to a low magnetic-moment state. The magnetization remains unchanged for further cooling until T_c(L) ≈ 120 K, below which a second magnetic transition occurs, causing a sudden jump to a high moment state. T_c(L) and T_c(H) do not change with x. There is an obscure but distinguishable maximum at ~ 180 K. It is a sign of an AFM transition as proved by neutron diffraction analysis (see the context). Therefore,

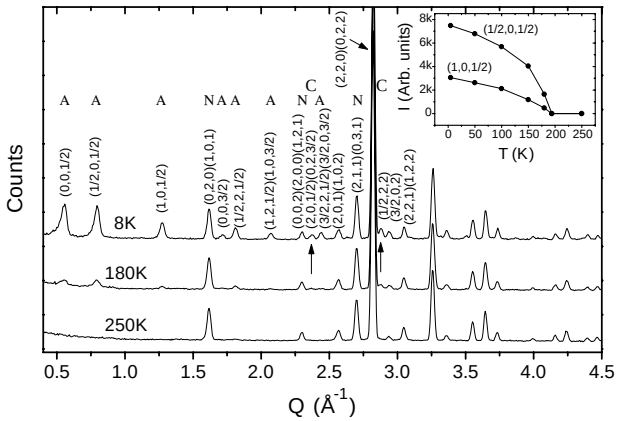

Fig. 2 – Neutron diffraction patterns of $La_{0.474}Bi_{0.193}Ca_{0.33}MnO_3$ collected at 8 K, 180 K, and 250 K ($\lambda = 1.66$ Å). Peaks corresponding to the nuclear reflections are marked by "N" and to the AFM reflections by "A". The inset displays the integrated intensities of the $(1/2, 0, 1/2)$ and $(1, 0, 1/2)$ peaks.

there are at least two possible phases below T_c(H): a FM phase and an AFM phase, the latter is a simultaneously charge-ordered phase. From the isothermal magnetization curve (right panel of fig. 1), the percentage of the FM phase in the two different magnetic states can be estimated. Extrapolating the Arrott plot in the inset to $H = 0$, we obtained the spontaneous magnetization, and it is $M_s \approx 18.1$ emu/g for LBCM8 at $T = 150$ K before the field-induced FM transition. The FM component is $\sim 22\%$ of the total population noting the fact that the spontaneous magnetization will be ~ 83.7 emu/g if all the phases are converted into the FM phase by an applied field. A similar calculation specifies that the FM fraction is $\sim 84\%$ at 5 K. Therefore, $\sim 60\%$ other phases are converted into the FM phase when the sample is cooled down from the low-moment state to the high-moment state. In contrast, the population of the FM phase increases by $\sim 20\%$ around the second magnetic transition in LBCM9.

To get further information on the AFM and CO transition, neutron diffraction was subsequently performed for LBCM9 ($\lambda = 1.66$ Å). In fig. 2 we show three selected powder patterns collected at 8 K, 180 K and 250 K, respectively. Only the nuclear reflections are observed above 250 K (labeled by "N"). When the sample is cooled below 180 K, additional peaks that can be indexed based on an AFM superlattice appear (the peaks with half-integer indices). *It is obvious that the CO and AFM transitions take place simultaneously.* Particularly, the $(h, k, l/2)$ peaks, l odd, are associated with the Jahn-Teller distortions characteristic of the CE-type charge and orbital ordered state according to Yoshizawa *et al.* [11] and Kiryukhin *et al.* [7]. This feature remains down to 8 K, the lowest temperature of this experiment. We calculated the intensity of the typical AFM peak $(1/2, 0, 1/2)$ and, fascinatingly, found no visible changes when the temperature goes through T_c(L) (inset in fig. 2). This is a result similar to that obtained by Kiryukhin *et al.* for $La_{0.275}Pr_{0.35}Ca_{0.375}MnO_3$, in which the population of the CO phase has been found unaffected across T_c(L) [7]. We did not perform the neutron diffraction study for LBCM8. However, considering the similar magnetic character of the two samples, this conclusion is expected to be applicable to LBCM8.

Based on the above results, the low-temperature transition cannot be an AFM-FM transition. An alternative possibility is that it is also a PM-FM transition: the remaining PM phase is converted into the FM phase. This in turn leads to a new question on whether the PM phase exists near T_c(L). To examine the phase constituent of LBCM8 and LBCM9, the ESR

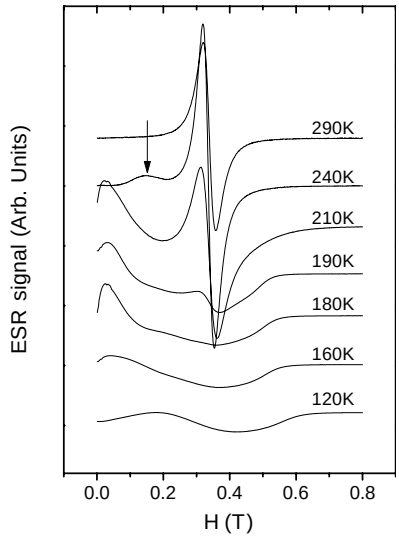

Fig. 3 – Electron spin resonance (ESR) spectra at different temperatures for $La_{0.67-x}Bi_xCa_{0.33}MnO_3$ ($x = 0.167$). The arrow in the figure indicates the resonance of the ferromagnetic phase.

spectra were measured for every 10 K in the range from 120 K to 300 K. The typical results for LBCM8 are presented in fig. 3 (similar results are obtained for LBCM9). It shows that the only detectable phase is the PM phase above 250 K. FM phase sets in at ~ 240 K, marked by a hump in the low-field region of the spectra, and its intensity increases with cooling. As a consequence, the PM signal decreases progressively and, finally, vanishes.

To get a quantitative description for the coexisting phases, the integrated ESR spectra have been calculated and fitted to Lorentzian functions (Gaussian functions were used when the temperature is below ~ 220 K) with adjustable resonance field, linewidth, and intensity (fig. 4). The absorption line above 250 K can be described satisfactorily by a single Lorentzian function centered at $H = 0.34$ T, which indicates the PM nature of the resonance. However, two absorption lines, respectively peaked at LF and HF, have to be used to reproduce the spectra below 240 K. The resonance peak around HF inherits all the characters of the PM line, and is a contribution of the PM component. HF shows a slight decrease with cooling, varying from ~ 0.34 T for $T = 240$ K to ~ 0.3 T for $T = 120$ K. It could be an effect of the internal field from the coexisting FM domains. In contrast, the LF line appears at a lower resonance field, generally below ~ 0.2 T, and has to be fitted by a Gaussian function. This resonance is usually ascribed to the FM phase in the literature [12]. *Contributions from the FAM phase cannot be detected under the present experimental conditions.* Compared with the PM line, the FM peak is much broader; this feature becomes increasingly obvious with the decrease of temperature, and part of it even extends to the negative field region. According to Kittle [13], the resonance field for an elliptical sphere is $H_r = \{[H_0+(N_x-N_z)H_m][H_0+(N_y-N_z)H_m]\}^{1/2}$ if the external field is applied along the z-axial, where N_x, N_y, and N_z are the demagnetization factors along the x, y and z axes, respectively, H_0 is the sum of the anisotropy and external fields, and H_m is the internal field associated with the magnetization of the FM phase. Due to the different demagnetization effects, anisotropy and internal fields, each kind of domain structure will yield a distinctive FM resonance [14]. It is instructive to note that the system does not get the saturation state before $H = 0.6$ T (fig. 1). Therefore, the magnetic domain structure could be

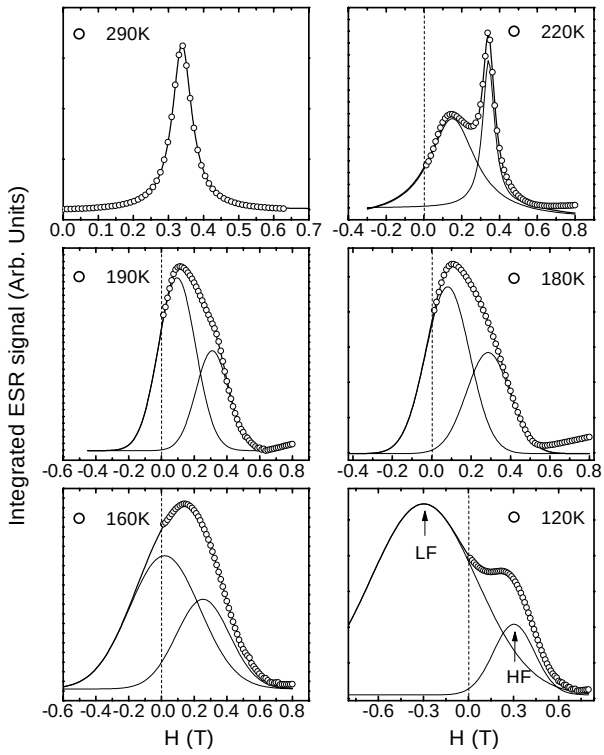

Fig. 4 – Integrated electron spin resonance (ESR) spectra at selected temperatures for $La_{0.67-x}Bi_xCa_{0.33}MnO_3$ ($x = 0.167$). Solid lines are fittings based on the Lorentzian/Gaussian functions. Two resonance lines marked by thin lines are required to fit the spectra below 240 K. The peak with a negative resonance field is a virtual resonance line, and only a part of it with $H > 0$ can be detected by ESR.

complex in the two-coexisting-phase compounds under low field. For example, a red-cabbage–like structure has recently been reported for the phase-separated $Pr_{0.67}Ca_{0.33}MnO_3$ [15]. As a consequence, H_0 will distribute in a wide range from $H_r - H_m$ to H_r when the frequency of the microwave field is fixed. To guarantee the occurrence of the FM resonance, it is demanded that $H_m < H_0$. This condition cannot be satisfied in some domains with large internal fields even without an external field. It means that part of the FM phase is invisible for the FM resonance. We represent the contribution of this part FM phase by the virtual resonance in the negative field region shown in fig. 4.

Compared with the resonance at HF, the position of the LF line shifts to low fields much faster with cooling (fig. 5). It reflects the rapid enhancement of the internal field: the decrease of temperature suppresses the thermal fluctuation of the spins. As a result, the FM resonance peak broadens systematically. This is understandable by noting that the depression of spin fluctuation will enhance H_m, thus widening the $H_r - H_m \to H_r$ range. This is consistent with the observations that the FM peak expands to the low fields while its high-field edge remains essentially unaffected (fig. 4). The significant broadening of the LF peak near ~ 120 K should be a consequence of the magnetic transition: the domain structure undergoes a rearrangement near $T_c(L)$. The second magnetic transition will finish at ~ 80 K. We cannot measure the FM resonance below 110 K due to, unfortunately, the limit of our experiment device.

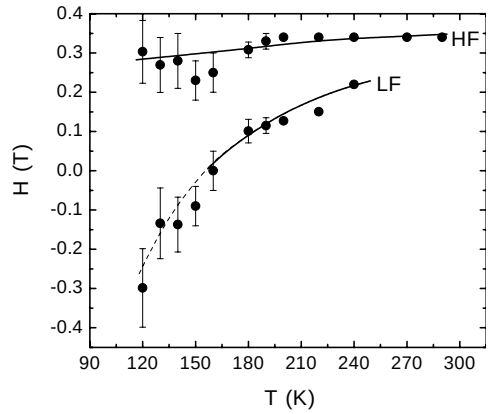

Fig. 5 – Resonance field against temperature for $La_{0.67-x}Bi_xCa_{0.33}MnO_3$ ($x = 0.167$). LF and HF are the resonance fields for the FM and PM phases, respectively. Solid and dashed lines are guides for the eye.

It is a natural assumption that the population of the PM/FM phase is proportional to the areas of the corresponding resonance peaks (S_{PM}/S_{FM}). From the FM line one can estimate the percentage of the FM phase detected by ESR (the virtual part of the FM peak is also included considering that we want the total contribution of the FM phase). Based on a simple calculation, the relative area of the PM phase $S_{PM}/(S_{PM} + S_{FM})$, which is closely related to the PM fraction in LBCM8, can be obtained, and the results are shown in fig. 6. $S_{PM}/(S_{PM} + S_{FM})$ is 100% above 250 K, and exhibits a steep decrease between 220 K and 240 K, corresponding to the emergence and development of the FM phase. It is $\sim 40\%$ in the range 150–190 K, and $\sim 20\%$ at 120 K. Therefore, a considerable amount of PM phase persists down to $\sim$ 120 K. This is in sharp contrast to $La_{0.67}Ca_{0.33}MnO_3$, in which the PM phase exists in a very narrow temperature region below T_c [9]. Compared with $La_{0.67}Ca_{0.33}MnO_3$, a special feature of LBCM8 is the coexistence of the FM and the CO AFM phases below T_c(H). It has been proved that the lattice undergoes an expansion in the *a*-*b* plane and a contraction

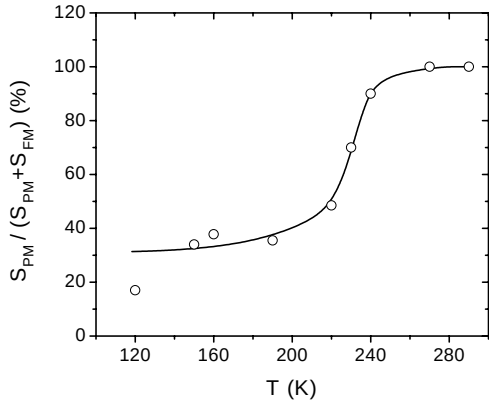

Fig. 6 – Relative area of the PM resonance peak as a function of temperature. The solid line is a guide for the eye.

along the c-axis when CO takes place, and the change in the lattice parameter can be as large as $\sim 0.3\%$ [16]. In contrast, *the lattice variation for a second-order PM-FM transition is small*. With this in mind, inhomogeneous strains are expected near the CO-FM interfaces due to the significant lattice mismatch [17, 18], and the PM phase most probably appears in those regions between the FM and the CO domains.

Based on the above studies on the magnetic property, ESR and neutron diffraction spectra, a complete scenario for the phase-separation in the LBCM series can be proposed: the PM phase dominates above 250 K, the PM and FM phases coexist between 240 K and 180 K. Below 180 K, part of the PM phase is changed into the CO AFM phase, and the three phases coexist until the second magnetic transition, which converts the remaining PM phase into the FM phase.

* * *

This work has been supported by the State Key Project of Elementary Research of China and the National Nature Science Foundation of China.

REFERENCES

[1] Rao G. H., Sun J. R., Liang J. K. and Zhou W. Y., *Phys. Rev. B*, **55** (1997) 3742.
[2] Ibarra M. R., Zhao G. M., De Teresa J. M., Garcia-Landa B., Arnold Z., Marquina C., Algarabel P. A., Keller H. and Ritter C., *Phys. Rev. B*, **57** (1998) 7446.
[3] Uehara M., Mori S., Chen C. H. and Cheong S.-W., *Nature (London)*, **399** (1999) 560.
[4] Kim K. H., Uehara M., Hess C., Sharma P. A. and Cheong S.-W., *Phys. Rev. Lett.*, **84** (2000) 2961.
[5] Podzorov V., Uehara M., Gershenon M. E., Koo T. Yo. and Cheong S.-W., *Phys. Rev. B*, **61** (2000) R3784.
[6] Niebieskikwiat D., Sanchez R. D. and Caneiro A., *J. Magn. & Magn. Mater.*, **237** (2001) 241.
[7] Kiryukhin V., Kim B. G., Podzorov V., Cheong S.-W., Koo T. Y., Hill J. P., Moon I. and Jeong Y. H., *Phys. Rev. B*, **63** (2000) 24420.
[8] Radaelli P. G., Ibberson R. M., Argyriou D. N., Casalta H., Andersen K. H., Cheong S.-W. and Mitchell J. F., *Phys. Rev. B*, **63** (2001) 172419.
[9] Liu N., Sun Y. and Zhang Y. H., *Chin. Phys. Lett.*, **18** (2001) 957.
[10] Blasco J., Garcia J., De Teresa J. M., Ibarra J. M., Algarabel P. A. and Marquina C., *J. Phys. Condens. Matter*, **8** (1996) 7427.
[11] Yoshizawa H., Kajimoto R., Kawano H., Tomioka Y. and Tokura Y., *Phys. Rev. B*, **55** (1997) 2729.
[12] Rivadulla F., Freita-Alvite M., Lopez-Quintela M. A., Hueso L. E., Miguens D. R., Sande P. and Rivas J., *J. Appl. Phys.*, **91** (2002) 785.
[13] Kittel C., *Introduction to Solid State Physics*, 5th edition (John Willey & Sons, Inc.) 1976.
[14] Morrish A. H., *The Principles of Magnetism* (IEEE, New York) 2001.
[15] Simon Ch., Mercone S., Guiblin N., Martin C., Brûlet A. and André G., *Phys. Rev. Lett.*, **89** (2002) 207202.
[16] Kuwahara H., Tomioka Y., Asamitsu A., Moritomo Y. and Tokura Y., *Science*, **270** (1995) 961.
[17] Kimura T., Tomioka Y., Kumai R., Kimoto Y. and Tokura Y., *Phys. Rev. Lett.*, **83** (1999) 3940.
[18] Mahendiran R., Raveau B., Herrien M., Michel C. and Maihnan A., *Phys. Rev. B*, **64** (2001) 064424.